

## Experimental and theoretical research on the compression performance of CFRP sheet confined GFRP short pole

Li Chen<sup>a</sup>, Qilin Zhao\* and Kebin Jiang<sup>b</sup>

Engineering Institute of Engineer Corps, PLA University of Science and Technology, Nanjing, China

(Received October 24, 2010, Revised May 24, 2011, Accepted August 17, 2011)

**Abstract.** The axial compressive strength of unidirectional FRP is generally quite lower than its axial tensile strength. This fact decreases the advantages of FRP as main load bearing member in engineering structure. In order to restrain the lateral expansion and splitting of GFRP, and accordingly heighten its axial compressive bearing capacity, a project that to confine GFRP pole with surrounding CFRP sheet is suggested in the present study. The Experiment on the CFRP sheet confined GFRP poles showed that a combined structure of high bearing capacity was attained. Basing on the experiment research a theoretical iterative calculation approach is suggested to predict the ultimate axial compressive stress of the combined structure, and the predicted results agree well with the experimental results. Then the influences of geometrical parameters on the ultimate axial compressive stress of the combined structure are also analyzed basing on this approach.

**Keywords:** CFRP; GFRP pole; confinement; compressive strength; experiment; iteration

---

### 1. Introduction

Compared with traditional materials, unidirectional FRP possesses the advantages of high axial tensile strength, lightness and corrosion resistance, etc. It can substitute steel as structural material in many tensile occasions, such as the external tendon of prestressed concrete bridge (Youakim and Karbhari 2007) and the main cable of cable-stayed bridge (Wang and Wu 2010). And it is also used for compression bearing members more and more widely, such as poles of light trusses (Xiong *et al.* 2010), falseworks (Hollaway 2010), and other infrastructures (Juran and Komornik 2006). Nevertheless, in general opinion, FRP poles are not fit to bear heavy compression load because of their low compressive stabilities and low compressive strengths. For instance, as showed by the experiment on FRP poles carried by Zhang *et al.* (2006), the compressive strengths of the CFRP (carbon fiber reinforced composite) poles and the GFRP (glass fiber reinforced composite) poles are only about 11% and 40% of their tensile strengths respectively when there are completely no lateral confinement. When buckling of FRP poles under heavy compression load is restrained by adopting

---

\*Corresponding author, Associate Professor, E-mail: zhaohs ql919@163.com

<sup>a</sup>Ph.D. Student, E-mail: alexandermacedonia@163.com

<sup>b</sup>Professor, E-mail: kbjiang@sina.com

hollow sections or setting lateral supports, the relatively low compression strengths may become the bottleneck for them to be used as main compression load bearing members in engineering structures.

Confining concrete members with CFRP sheet externally to enhance the compressive strength and ductility of the concrete is a widely adopted engineering technology currently (Zhang *et al.* 2009, Woo *et al.* 2010). It is based on the following mechanism: the concrete expands laterally when axially compressed, and this will drive the surrounding CFRP sheet to apply lateral confinement to the concrete consequently, which in turn restrains the lateral expansion and cracking of the concrete, so the compressive strength of concrete is heightened. Analogously, experiments have showed that the axial compressive strength of unidirectional FRP can also be enhanced by lateral pressure applied on it (Hoppel and Bogetti 1995). For a kind of carbon/epoxy composite, its axial compressive strength increases by about 400 MPa when the hydrostatic pressure increases from 100 MPa to 500 MPa (Weaver and Williams 1975). For a kind of glass/epoxy composite, its axial compressive strength increases by about 900 MPa when the hydrostatic pressure increases from 50 MPa to 300 MPa (Wronski and Parry 1982). So basing on the specialty of unidirectional FRP that the axial compressive strength increases with hydrostatic pressure, referring the idea of CFRP sheet confined concrete, the project that to confine GFRP pole with surrounding CFRP sheet is suggested, with the expectation that to restrain the lateral expansion and splitting of the GFRP pole, and accordingly heighten its axial compressive bearing capacity. Experiment research on CFRP sheet confined GFRP poles was carried out to study the mechanism and regularity for CFRP sheet to heighten the compressive strength of the GFRP poles. A theoretical iterative calculation approach is suggested to predict the ultimate compressive stress of the combined structure and then the factors influencing the ultimate compressive stress are analyzed on the basis of this approach.

## 2. Experiment

### 2.1 Experiment process

5 groups of CFRP sheet confined GFRP short pole specimens were compressed.

The CFRP sheet was produced by stitching tows of a high modulus carbon fiber unidirectionally, and the nominal thickness of the sheet layer is 0.167 mm. The GFRP poles were molded from epoxy resin and e-glass fiber. The glass fibers were all laid in the axial direction of the poles. The cross section of the poles was a solid cycle with the diameter of 50 mm. The GFRP poles were then cut into 100 mm long. The carbon fiber sheet was cut along the laying direction of the fiber into strips, of which the width was equal to the length of the short poles, and then wrapped outside the surface of the short poles after dipped to the adhesive. The CFRP sheet confined GFRP poles were finally finished after room temperature solidification of the adhesive. The measured initial mechanical parameters of the resin and the mechanical parameters of the glass fiber and carbon fiber are showed in Table 1.

The specimens were grouped as Group 1, Group 2, Group 3, Group 4 and Group 5 by the layer numbers of surrounding CFRP sheet. Group 1 were unconfined GFRP short poles, and the other 4 groups were CFRP sheet confined GFRP poles, with 2, 4, 6 and 8 layers of CFRP sheet respectively. 5 specimens were chose as available specimens from each group according test results.

The experiment was executed on a 200 t compression testing machine. In the experiment, the data

Table 1 Data of the raw materials

Data	Elastic modulus (GPa)	Poisson ratio	Volume fraction (%)
Epoxy resin	3.3	0.369	0.6
e-glass fiber	85.0	0.5	0.4
High modulus carbon fiber	700	-	-

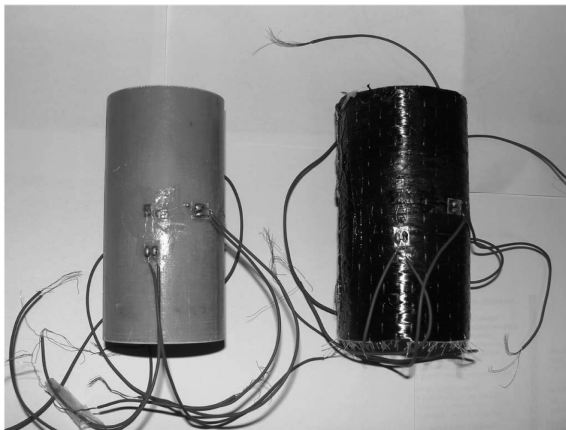


Fig. 1 Unconfined GFRP short pole specimen and CFRP sheet confined GFRP short pole specimen

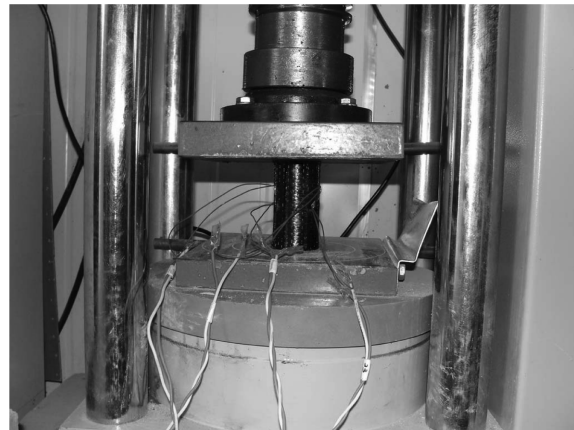


Fig. 2 Axial compressive loading situation

of compressive load, the axial strain and the lateral strain was collected; the failure phenomenon was observed and recorded. The compressive load was directly read from the LCD of the testing machine. Each 2 strain gages which were laid transversely or axially were glued on the middle part of the specimen surface to get the strain values, and the values were then transmitted to a computer by a data acquisition system. The transverse and the axial strain gages were both laid symmetrically to the axis of the pole, in order to counteract the error induced by eccentricity. The specimens were loaded with step loading. Part of the prepared specimens and the loading situation is showed in Fig. 1 and Fig. 2 respectively.

## 2.2 Failure phenomenon

The unconfined GFRP short pole specimens gave a suddenly crepitation as the load reached the ultimate value, and the load value decreased significantly at the same time, which was showed by the LCD. It could be seen that there were penetrating splits in the surfaces of the specimens. So the specimens was realized to be failed and the loading was terminated. The typical failure mode was the transverse splitting of GFRP, as showed by Fig. 3.

The CFRP sheet confined GFRP short pole specimens gave a suddenly crepitation as the load reached the ultimate value, and the load value decreased significantly at the same time. The CFRP sheet ruptured and the core GFRP poles split more thoroughly than in the unconfined situation. The specimens were realized to be failed and the loading was terminated. The typical failure mode was rupture of the CFRP sheet and the subsequent transverse splitting of the GFRP, as showed by Fig. 4.

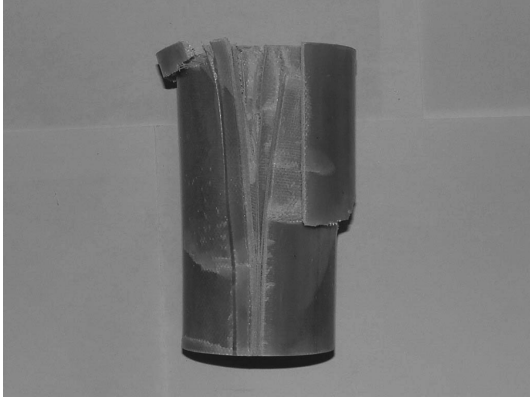


Fig. 3 Compressing failed unconfined GFRP short pole

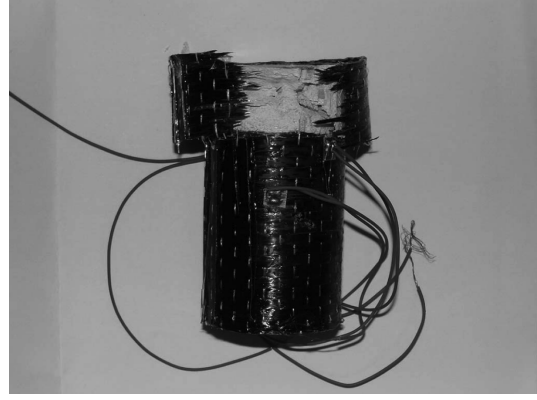


Fig. 4 Compressing failed CFRP sheet confined GFRP short pole

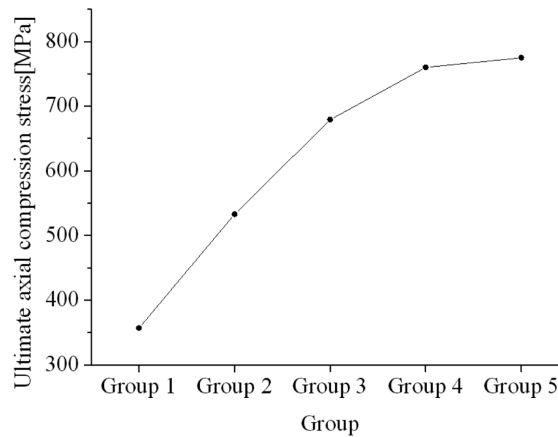


Fig. 5 Average ultimate axial compressive stress of different groups of specimens

### 2.3 Ultimate axial compressive stress

The presence of the surrounding CFRP sheet significantly increases the ultimate axial compressive stress of the GFRP pole, as showed in Fig. 5. Since the differences between the CFRP layer numbers of arbitrary two adjacent group specimens are equal, it is clear that the ultimate stress of specimen presented a nonlinear increasing trend as the total thickness of CFRP sheet layers increases. When the surrounding CFRP sheet increases from 0 layer (Group 1) to 2 layers (Group 2), the average ultimate stress of the specimens increases by 176 MPa. Yet when the surrounding CFRP sheet increases from 6 layers (Group 4) to 8 layers (Group 5), the average ultimate stress of the specimens increases by only 13 MPa. As the initial total thickness of CFRP sheet layers increases, the heightening effect of CFRP thickness increase to the ultimate stress of the combined structure decreases.

### 2.4 Mechanical behavior of CFRP sheet confined GFRP short pole

The macroscopic failure mode of unconfined GFRP short pole tends to be transverse splitting.

When CFRP sheet confined GFRP pole is axially compressed, it expands laterally because of Poisson ratio effect. This causes circumferential tensile strain and stress in the CFRP sheet, and then the CFRP sheet applies lateral pressure to the GFRP pole conversely. When the axial compressive load increases, the circumferential stress in the CFRP sheet increases with the lateral expansion strain of the GFRP, and the confining pressure to the GFRP pole increases accordingly until the CFRP sheet ruptures. Though the load applied on the combined structure is uniaxial, the GFRP pole surrounded by CFRP sheet is under multiaxial compression, namely is affected by the axial load and the lateral confining pressure, of which the latter depends on the former. In this stress state of multiaxial compression, the matrix of the GFRP is stiffened, and the microbuckling, which is generally considered to be the main origin of GFRP compression failure, is restrained. Moreover, the lateral expansion and the transverse splitting of the whole pole is restrained. So the ultimate compressive stress of the pole is heightened. The interaction between the CFRP sheet and the GFRP pole is the basis for the two to cooperate and for the GFRP to be enhanced.

Before the CFRP sheet ruptures, the axial compressive load applied on the confined GFRP pole has exceeded the ultimate load value in the unconfined situation, and the GFRP has reached the critical state of splitting. It does not fail just because that the confinement from CFRP restrained the formation of macroscopic transverse splits in it. Once the CFRP sheet ruptured, the strain energy which is cumulated in the GFRP is released instantly and the pole splits at the same time.

### 3. Theoretical calculation approach of ultimate compressive stress

CFRP sheet is a linear elastic material in the direction which the fiber lays in. Similar to other kinds of fibers, its mechanical parameters can be considered to be insensitive to the stress state. In general condition, GFRP can be seen as a linear elastic material in the fiber direction, but under non-axial stresses it has a nonlinear performance (Zinoviev *et al.* 2001, Hine *et al.* 2005, Gonzalez and Lorca 2007). That is because in the two phases of materials that compose GFRP, the mechanical parameters of fiber cannot be affected by the stress state, yet those of the resin are sensitive to the stress state (Hoppel and Bogetti 1995). When the CFRP sheet confined GFRP pole is axially loaded, the variation of stress state causes variation of the resin mechanical parameters, and accordingly variation of the GFRP mechanical parameters.

As the mechanical parameters of GFRP are functions of stress state, an iterative calculation approach considering variation of the GFRP mechanical parameters with stress state is suggested to predict the ultimate axial compressive stress of CFRP sheet confined GFRP.

#### 3.1 Elastic mechanics model

The equilibrium differential equations in cylindrical coordinate system (Xu 1990)

$$\begin{cases} \frac{\partial \sigma_r}{\partial r} + \frac{\partial \sigma_{zr}}{\partial r} + \frac{\sigma_r - \sigma_\theta}{r} = 0 \\ \frac{\partial \sigma_z}{\partial z} + \frac{\partial \sigma_{rz}}{\partial r} + \frac{\sigma_{rz}}{r} = 0 \end{cases} \quad (1a, b)$$

The geometric equations in cylindrical coordinate system (Xu 1990)

$$\left\{ \begin{aligned} \varepsilon_r &= \frac{\partial u_r}{\partial r} \\ \varepsilon_\theta &= \frac{u_r}{r} \\ \varepsilon_z &= \frac{\partial w}{\partial z} \\ \gamma_{zr} &= \frac{\partial u_r}{\partial z} + \frac{\partial w}{\partial r} \end{aligned} \right. \quad (2a, b, c, d)$$

Unidirectional GFRP is a transversely isotropic material. This mechanical characteristic should be taken into consideration when the elastic mechanics model of CFRP sheet confined GFRP pole is being established. The GFRP pole physical equations in the cylindrical coordinate system can be attained by treat that in the rectangular coordinate system (Jones 1975) with coordinate transformation (Fung 1994)

$$\begin{bmatrix} \varepsilon_z \\ \varepsilon_r \\ \varepsilon_\theta \\ \varepsilon_{r\theta} \\ \varepsilon_{\theta z} \\ \varepsilon_{zr} \end{bmatrix} = \begin{bmatrix} \frac{1}{E_1} & -\frac{\nu_{12}}{E_2} & -\frac{\nu_{12}}{E_2} & 0 & 0 & 0 \\ -\frac{\nu_{12}}{E_2} & \frac{1}{E_2} & -\frac{\nu_{23}}{E_2} & 0 & 0 & 0 \\ \frac{\nu_{12}}{E_2} & -\frac{\nu_{23}}{E_2} & \frac{1}{E_2} & 0 & 0 & 0 \\ 0 & 0 & 0 & 2\left(\frac{1}{E_2} + \frac{\nu_{23}}{E_2}\right) & 0 & 0 \\ 0 & 0 & 0 & 0 & \frac{1}{G_{12}} & 0 \\ 0 & 0 & 0 & 0 & 0 & \frac{1}{G_{12}} \end{bmatrix} \begin{bmatrix} \sigma_z \\ \sigma_r \\ \sigma_\theta \\ \sigma_{r\theta} \\ \sigma_{\theta z} \\ \sigma_{zr} \end{bmatrix} \quad (3a)$$

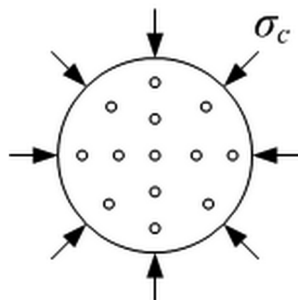


Fig. 6 Core GFRP pole affected only by the lateral confining pressure

Suppose that the core GFRP pole is only affected by the lateral confining pressure  $\sigma_c$  without axial compressive stress (Fig. 6). The stress field boundary conditions are

$$\begin{cases} \sigma_z = 0 \\ \sigma_{zr} = \sigma_{rz} = 0 \\ \sigma_r|_{r=R} = \sigma_C \\ \sigma_r|_{r=0} = \sigma_\theta|_{r=0} \end{cases} \quad (4a, b, c, d)$$

Where  $R$  is the radius of the pole section. Then from Eq. (3a) we get

$$\begin{cases} \varepsilon_r = \frac{\sigma_r - \nu_{23}\sigma_\theta}{E_2} \\ \varepsilon_\theta = \frac{\sigma_\theta - \nu_{23}\sigma_r}{E_2} \end{cases} \quad (3b, c)$$

Exert Eq. (4b), and Eq. (1a) can be simplified as

$$\frac{\partial \sigma_r}{\partial r} + \frac{\sigma_r - \sigma_\theta}{r} = 0 \quad (1c)$$

According to Eq. (2a) and Eq. (2b), the deformation compatibility equation can be derived as

$$\frac{\partial \varepsilon_\theta}{\partial r} + \frac{\varepsilon_\theta - \varepsilon_r}{r} = 0 \quad (2e)$$

Exert Eq. (3) to express the strains  $\varepsilon_\theta$  and  $\varepsilon_r$  in Eq. (2e) with stresses, then simplify it with Eq. (1c), and the following equation can be attained

$$\frac{\partial(\sigma_r + \sigma_\theta)}{\partial r} = 0 \quad (2f)$$

Combine Eq. (1c) and Eq. (2c) and solve the simultaneous differential equations, then we get

$$\begin{cases} \sigma_r = C_1 + \frac{C_2}{r^2} \\ \sigma_\theta = C_1 - \frac{C_2}{r^2} \end{cases} \quad (5a, b)$$

By substituting Eq. (5a, b) to Eq. (4d) we get

$$C_2 = 0 \quad (4e)$$

By substituting Eq. (5a) and Eq. (4e) to Eq. (4c) we get

$$C_1 = \sigma_C \quad (4f)$$

Consequently we get

$$\sigma_r = \sigma_\theta = \sigma_c \quad (5c)$$

When the axial compressive pressure  $q$  is applied to the combined structure, the radial deformation of the core GFRP pole is composed by two parts, of which one is the deformation  $u_{rC}^F$ , caused only by the lateral confining pressure from the CFRP sheet, the other is the deformation  $u_{rq}^F$ , caused only by the axial compressive load. The radial deformation  $u_r^C$  of the CFRP sheet internal surface is equal to the radial deformation of GFRP pole external surface, and this relation can be written as

$$u_{rC}^F + u_{rq}^F = u_r^C \quad (6)$$

Firstly only the affection of lateral pressure  $\sigma_c$  on GFRP pole is considered. According to Eq. (3b) and Eq. (5c) we have

$$\varepsilon_{rC}^F = \frac{\sigma_c(1 - \nu_{23})}{E_2} \quad (7a)$$

Where  $\varepsilon_{rC}^F$  is the strain of GFRP pole caused only by the lateral confining pressure. Consequently we get

$$u_{rC}^F = \int_0^R \varepsilon_{rC}^F dr = \frac{\sigma_c R(1 - \nu_{23})}{E_2} \quad (8a)$$

Then only the affection of axial pressure  $q$  is considered, and we have

$$\varepsilon_{rq}^F = -\frac{\sigma_z \nu_{12}}{E_2} \quad (7b)$$

Where  $\varepsilon_{rq}^F$  is the strain of GFRP pole caused only by the axial compressive load. Consequently we get

$$u_{rq}^F = -\frac{\sigma_z R \nu_{12}}{E_2} \quad (8b)$$

By force equilibrium of the CFRP sheet we have

$$\sigma_c = -\frac{\sigma_{tension} t}{R} \quad (9)$$

Where  $\sigma_{tension}$  is the tensile stress in the CFRP sheet, and  $t$  is the total nominal thickness of the CFRP sheet layers. The radial deformation of CFRP can be written as

$$R \frac{\sigma_{tension}}{E_{cf}} + \frac{1}{2} t \nu_{cf} \frac{\sigma_{tension}}{E_{cf}} = -\frac{\sigma_c R^2}{t E_{cf}} \left( 1 + \frac{t \nu_{cf}}{2R} \right) \quad (8c)$$

Where  $E_{cf}$  and  $\nu_{cf}$  is respectively the elastic modulus and the lateral Poisson ratio of the CFRP sheet. In general situation, because that the value of  $t \nu_{cf} / 2R$  is much smaller than 1, it can be approximately considered that

$$u_r^c = \frac{\sigma_c R^2}{t E_{cf}} \tag{8d}$$

Substitute Eq. (8a, b, d) to Eq. (6) and we get

$$\sigma_c = \frac{\nu_{12} q E_{cf} t}{R E_2 + E_{cf} t (1 - \nu_{23})} \tag{10}$$

According to Eq. (5c) and Eq. (10) the internal stress field of the GFRP pole can be summarized as following

$$\begin{cases} \sigma_r = \sigma_\theta = \sigma_c = \frac{\nu_{12} q E_{cf} t}{R E_2 + E_{cf} t (1 - \nu_{23})} \\ \sigma_z = q \end{cases} \tag{11a, b}$$

By substituting Eq. (11a, b) to Eq. (3a) the strain field of the pole can be calculated as

$$\begin{cases} \varepsilon_\theta = -\frac{\nu_{12} q R}{R E_2 + E_{cf} t (1 - \nu_{23})} \\ \varepsilon_r = -\frac{\nu_{12} q R}{R E_2 + E_{cf} t (1 - \nu_{23})} \\ \varepsilon_z = -\frac{q(-R E_2^2 - E_2 E_{cf} t + E_2 E_{cf} t \nu_{23} + 2 \nu_{12}^2 E_{cf} t E_1)}{(R E_2 + E_{cf} t - \nu_{23} t E_{cf}) E_1 E_2} \end{cases} \tag{12a, b, c}$$

As showed by Eq. (12a), the circumferential strain  $\varepsilon_\theta$  is a constant value anywhere in the confined GFRP pole, and is equal to the circumferential strain of the CFRP sheet.

### 3.2 Nonlinear property of GFRP

The elastic mechanics model of CFRP sheet confined GFRP pole is established and the stress and strain fields are calculated above. Yet the above model is based on the assumption that the GFRP material is always linear elastic, without considering the nonlinear property under multiaxial compression of GFRP. Thereby the calculated results by this model are not accurate enough. In order to attain more accurate results, the affection of multiaxial compression on the mechanical properties of GFRP should be taken into consideration.

The existing research results about GFRP mechanical properties in multiaxial stress state are mainly concerning the axial modulus, the strength and the failure mode etc., but there are few research results concerning the other aspects of mechanical properties (such as transverse modulus, Poisson ratio). Comparatively, the research results about the affection of multiaxial stress state on the mechanical properties of resin are more comprehensive (Pae and Sauer 1970, Christiansen and Baer *et al.* 1971, Silano and Bhateja *et al.* 1974, Pae and Bhateja 1975). For instance, Birch has derived the functional relations between the mechanical parameters of resin and the mutiaxial stress (Birch 1938). Meanwhile, mechanical properties of GFRP can be calculated by semi-empirical composition formulas from the mechanical properties of resin and fiber (Wang 1991). The calculation accuracy of these formulas has been testified to some extent.

To attain the mechanical parameters of GFRP in certain stress state, the mechanical parameters of resin in this state will be calculated primarily from its initial mechanical parameters, and then the mechanical parameters of the GFRP in the same stress state will be calculated with the composition formulas from the mechanical parameters of the fiber and that of the resin, which is calculated above.

As illuminated above, the mechanical parameters of glass fiber can be considered to be insensitive to the stress state.

The mechanical parameters of resin vary with stress state. The mechanical parameters of resin in certain stress state can be calculated by the formulas suggested by Birch (1938)

$$\begin{cases} E_m(P) = E_m + P[2(5 - 4\nu_m)(1 - \nu_m)] \\ G_m(P) = G_m + P \frac{3(3 - 4\nu_m)}{(1 + \nu_m)} \\ \nu_m(P) = \nu_m + \frac{P(1 + \nu_m)(-1 + 2\nu_m)(-1 + 4\nu_m)}{E_m \nu_m} \end{cases} \quad (13a, b, c)$$

Where  $-P = \sigma_{11} + \sigma_{22} + \sigma_{33}/3$ ;  $-P$  is the hydrostatic pressure;  $E_m$ ,  $G_m$  and  $\nu_m$  is respectively the initial value of the elastic modulus, the shear modulus and the Poisson ratio of the resin.

The mechanical parameters of GFRP can be calculated by the semi-empirical composition formulas as following (Wang 1991)

The axial modulus  $E_1$  and the transverse modulus  $E_2$

$$E_1 = E_{f1}V_f + E_mV_m \quad (14a)$$

$$E_2 = \frac{E_{f2}E_m(V_f + \eta_2V_m)}{V_fE_m + \eta_2V_mE_{f2}} \quad (14b)$$

$$\text{Where } \eta_2 = \frac{0.2}{1 - \nu_m} \left( 1.1 - \sqrt{\frac{E_m}{E_{f2}}} + \frac{3.5E_m}{E_{f2}} \right) (1 + 0.22V_f)$$

The shear moduli  $G_{12}, G_{23}$

$$G_{12} = \frac{G_{f12}G_m(V_f + \eta_{12}V_m)}{V_fG_m + \eta_{12}V_mG_{f12}} \quad (14c)$$

$$G_{23} = \frac{G_{f23}G_m(V_f + \eta_{23}V_m)}{V_fG_m + \eta_{23}V_mG_{f23}} \quad (14d)$$

$$\text{Where } \eta_{12} = 0.28 + \sqrt{\frac{E_m}{E_{f2}}}, \text{ and } \eta_{23} = 0.388 - 0.665 \sqrt{\frac{E_m}{E_{f2}}} + 2.56 \frac{E_m}{E_{f2}}.$$

The Poisson ratios  $\nu_{21}, \nu_{12}, \nu_{23}$

$$v_{21} = v_{f21}V_f + v_m V_m \quad (14e)$$

$$v_{12} = \frac{v_{21}E_2}{E_1} \quad (14f)$$

$$v_{23} = k(v_{f23}V_f + v_m V_m) \quad (14g)$$

Where  $k = 1.095 + (0.8 - V_f) \left[ 0.27 + 0.23 \left( 1 - \frac{E_{f2}}{E_{f1}} \right) \right]$ .

### 3.3 Iterative process

The iterative process consists of two steps, and is realized by programming on the computer. With the iterative process the stress and strain fields in the CFRP sheet confined GFRP pole under any axial compressive load can be calculated. Then the ultimate load of the combined structure can be detected by calling the iterative process and the selected failure criterion.

The first step. The axial pressure  $q$  is given. The initial value of lateral confining pressure  $\sigma_c$ , which is applied on the GFRP pole by the CFRP sheet, is set to be zero, and then the new value of  $\sigma_c$ , the stresses and strains in the combined structure are calculated. The new value and initial value of  $\sigma_c$  is compared. If the absolute value of the difference between the two is not more than a set tolerance, the iterative process is terminated. Otherwise the mechanical parameters of the resin are calculated with Eq. (13), and then the mechanical parameters of the GFRP are calculated with Eq. (14), with the new  $\sigma_c$  used in the calculation; then  $\sigma_c$ , the stresses and the strains is recalculated with Eq. (10), Eq. (11) and Eq. (12), using the new mechanical parameters of the GFRP. The above process is iterated until the absolute value of the difference between the last two  $\sigma_c$  values is not more than the above mentioned tolerance. And the last  $\sigma_c$  value is the exact confining pressure according the axial pressure  $q$ . Then the exact stress and strain fields of the combined structure and the exact mechanical parameters of the GFRP can be calculated. As showed by the above experiment research, the compression failure of CFRP sheet confined GFRP short pole is controlled by the rupture of the surrounding CFRP sheet. Thus the rupture of the CFRP sheet is seen as the sign of the combined structure to fail, and the maximum strain criterion is used to judge the rupture of CFRP. If  $\varepsilon_\theta$  does not exceed the ultimate strain of the CFRP sheet  $[\varepsilon_{carbon}]$ , the combined structure is realized to be not failed; otherwise it is realized that the CFRP sheet is ruptured and the combined structure is failed.

The second step. By calling the above iterative process the ultimate load of the combined structure can be calculated. The value of the compressive load  $q$  is increased continuously by a suitable pace, and accordingly the circumferential strain of the CFRP sheet can be calculated by the above approach. The  $q$  when the circumferential strain of the CFRP sheet achieves its rupture strain  $[\varepsilon_{carbon}]$  is compared with the ultimate compressive stress  $[q]_{unconfined}$  of the unconfined GFRP pole, and the major one is regarded as the combined structure ultimate compressive stress  $[q]$ .

The iterative process is illuminated with Fig. 7.

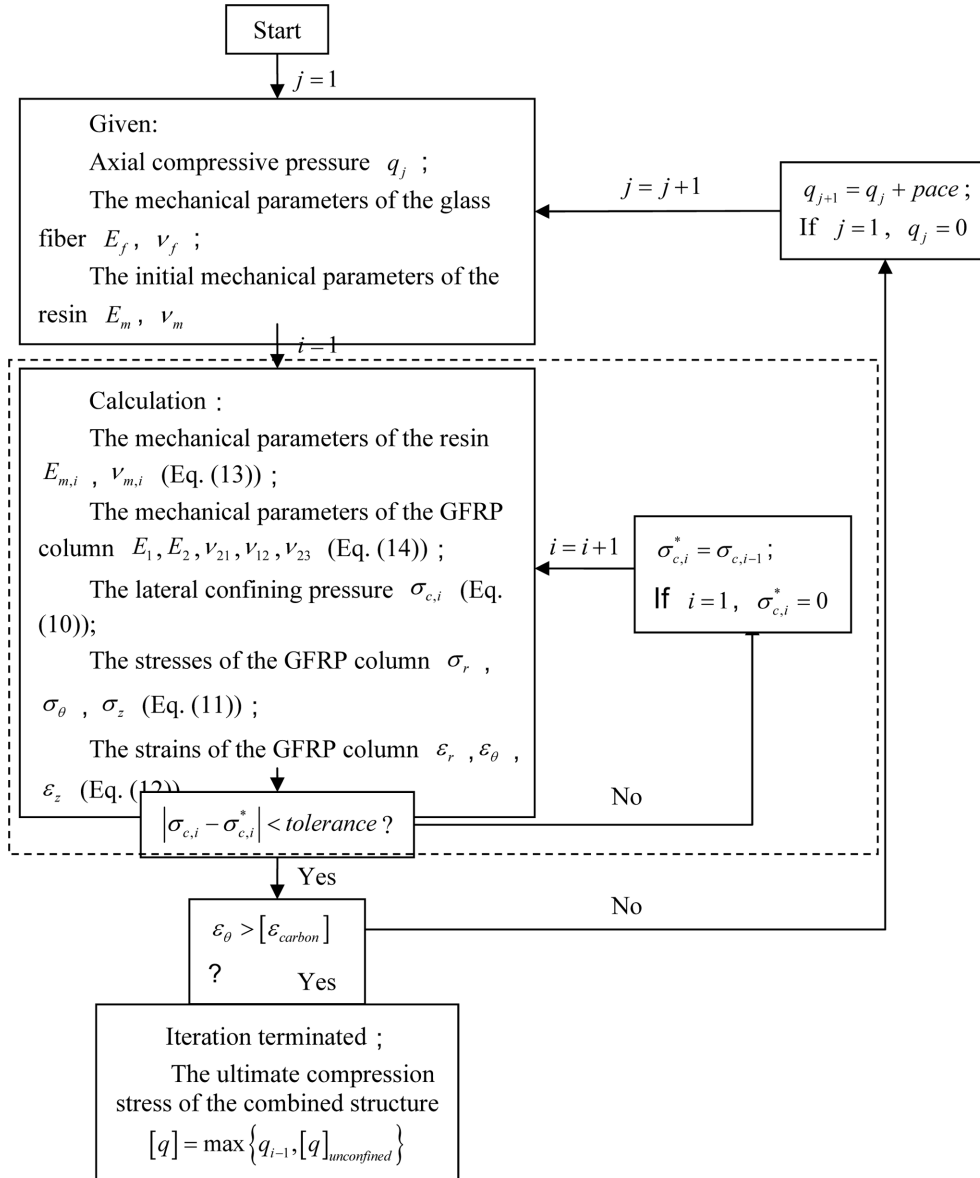


Fig. 7 Iterative calculation process for the ultimate compressive stress of the CFRP sheet confined GFRP short pole

#### 4. Theoretical-experimental comparison

##### 4.1 Stress-strain relations

The theoretical predicted axial strain  $\epsilon_z$  versus axial pressure  $q$  curve of each specimen group is compared with the typical experimental result of the group in Fig. 8. Because that the curves of

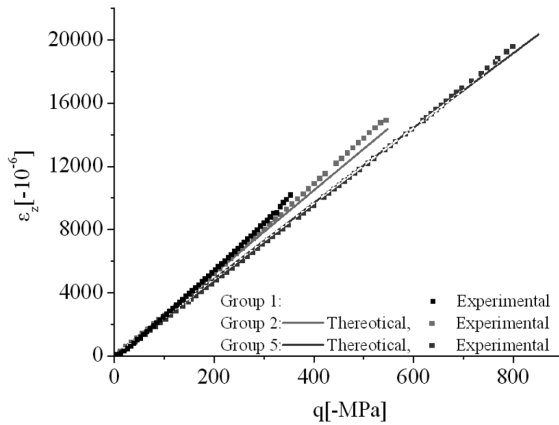


Fig. 8 Comparison between the theoretical and the typical experimental results on the  $\varepsilon_z$ - $q$  relation of different groups

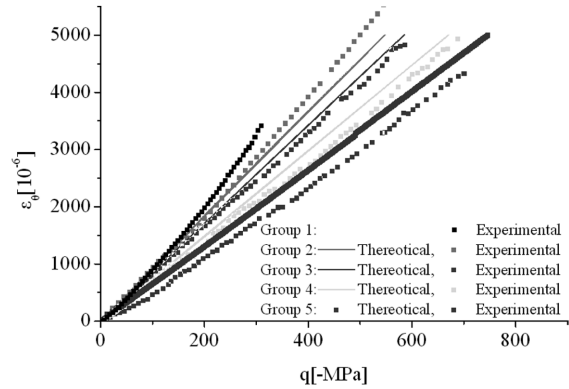


Fig. 9 Comparison between the theoretical and typical experimental results of different groups on the  $\varepsilon_\theta$ - $q$  relation

different groups are close to each other, for the purpose of clearness, only the results of Group 1, Group 2 and Group 5 are given. For Group 1 only the experimental result is given. For the other two groups the theoretical and the experimental results are given. The predicted responses agree well with the experimental results. There is just a little difference among the curves of the three groups. This illuminates that comparing to Group 1 (0 layer of CFRP sheet), the axial modulus  $E_1$  of Group 2 (2 layers of CFRP sheet) and Group 5 (4 layers of CFRP sheet) change very little. And it is proved that the presence of CFRP sheet has little effect on the axial modulus of the GFRP pole.

Fig. 9 shows the comparison between the theoretical and typical experimental results of different group specimens on the circumferential strain  $\varepsilon_\theta$  versus axial pressure  $q$  relation. For Group 1 only the experimental result is given, for the other 4 groups the theoretical and the experimental results are given. It can be seen that the theoretical results agree well with the experimental results. As indicated above, the lateral strain increase rate of the GFRP decreases gradually when the axial pressure increases, thus the  $\varepsilon_\theta$ - $q$  curves should be flexural convex curves. Yet because the curvatures of the curves are very small, this is not obvious in Fig. 9. Comparing different group specimen curves and it can be seen that the curve slopes of the specimens with more CFRP sheet are obviously smaller than those of the specimens with less CFRP sheet. This illuminates that the presence of the CFRP sheet restrains the lateral expansion of the GFRP pole effectively.

#### 4.2 Ultimate compressive stress

One of the key factors affecting the predicted value of the combined structure ultimate compressive stress is the selected value for the CFRP rupture strain. For the CFRP sheet confined GFRP pole, because of the factors such as local stresses and brittleness of the CFRP sheet induced by the solidification, the actual rupture strain of CFRP sheet is often less than the measured value attained by tensile test of carbon fiber (Lam and Teng 2003). Similar phenomenon is observed in this research, namely that the actual rupture stain of the carbon fiber sheet measured at the compression experiment is less than the measured value attained by tensile test of carbon fiber.

Table 2 Comparison between the experimental results and the theoretical values of the ultimate axial compressive stresses

Group number	Group 1	Group 2	Group 3	Group 4	Group 5
Average experimental value of 5 available specimens (MPa)	357	533	679	762	775
Theoretical value (MPa)	-	548	645	740	823
Error	-	+2.8%	-5.0%	+3.0%	+6.2%

Basing on the results of pretest, 0.0051 is adopted as the value of the CFRP sheet rupture strain [ $\varepsilon_{carbon}$ ]. The predicted ultimate axial compressive stresses of the different groups are listed in Table 2. The theoretical values agree well with the experimental results.

## 5. Influence of geometrical parameters on the ultimate stress

When the combined structure is loaded axially, it is in the plain strain state, so its stress and strain distribution cannot be affected by the pole height, and the geometrical parameters which affecting the stress and strain distribution and its ultimate axial compressive stress are merely the section radius  $R$  of the pole and the total thick  $t$  of the CFRP sheet layers.

### 5.1 $R$ varying proportionally with $t$

The predicted relations for the ultimate axial compressive stress  $[q]$  versus the section radius  $R$  when  $R/t$  are different constants is showed by Fig. 10. For 4 different  $R/t$  values, the ultimate stresses when  $R$  varies proportionally with  $t$  are calculated. The 5 data points on each curve denote  $[q]$  for GFRP poles of different  $R$  when  $R/t$  is a constant. It can be observed that when the material properties are ascertained, as long as  $R/t$  fixes to a constant, the ultimate axial compressive stress  $[q]$  keeps being a constant, no matter how  $R$  or  $t$  varies. Variation of  $R$  or  $t$  causes the variation of  $[q]$  by causing the variation of  $R/t$  firstly. In addition,  $[q]$  is a decreasing function of  $R/t$ .

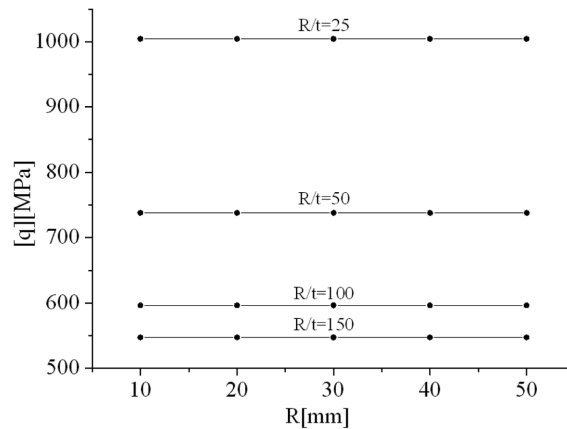


Fig. 10  $[q]$ - $R$  relation of the CFRP sheet confined GFRP pole when  $R/t$  are constants

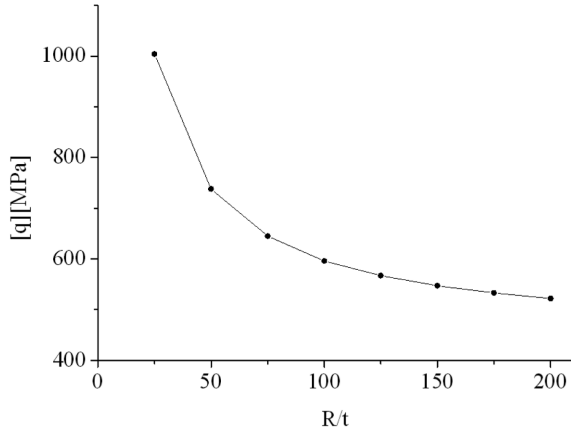


Fig. 11 [q]-R/t relation of the CFRP sheet confined GFRP pole

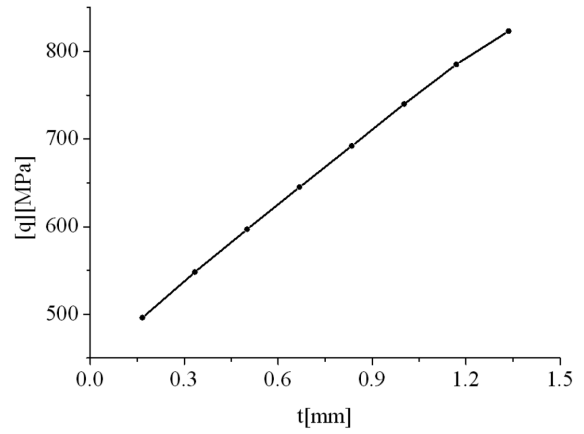


Fig. 12 [q]-t relation of the CFRP sheet confined GFRP pole when R is kept to 50 mm

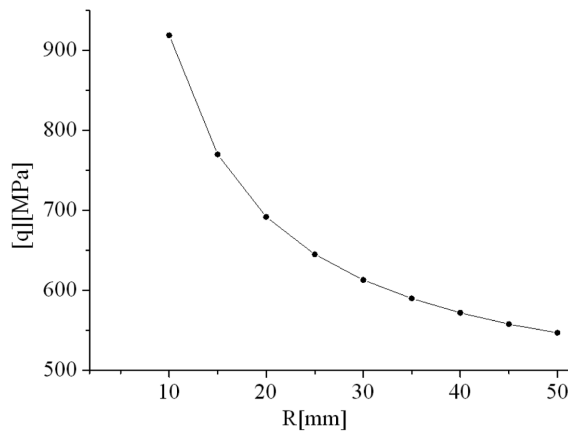


Fig. 13 [q]-R relation of the CFRP sheet confined GFRP pole when t is kept to 0.334 mm

### 5.2 R varying disproportionately with t

The predicted relation for [q] versus R/t is showed in Fig. 11, in which the 8 data points denote [q] at different R/t values. When R/t increases, [q] decreases gradually, and the curve tends to become horizontal. This indicates that the decrease tendency is weakening. The larger R/t is, the lower the sensitivity of [q] to the variation of R/t is. It is easy to be inferred that, when R/t tends to infinity, [q] will tend to the axial compressive strength of the unconfined GFRP short pole.

The predicted relation for [q] versus t when R is 50 mm is showed in Fig. 12, and the predicted relation for [q] versus R when t is 0.334 mm (which is equal to the thickness of 2 layers of CFRP sheet) is showed in Fig. 13. When R or t varies separately, [q] increases with the increase of t or the decrease of R, and decreases with the decrease of t or the increase of R.

## 6. Conclusions

The confinement of CFRP restrains the transverse deformation and splitting of the GFRP pole under axial compressive load, and heightens the axial compressive strength of the GFRP effectively. With the increasing of the total thickness of the confining CFRP sheet, the ultimate compression stress of the combined structure presents a nonlinear increasing trend. The lateral expansion of the core GFRP pole causes interaction between the GFRP pole and CFRP sheet, and this is the basis for the GFRP to be confined and enhanced. When the circumferential strain of the CFRP sheet achieves its rupture strain, the CFRP sheet will rupture and the GFRP pole will transversely split consequently. In this situation, the rupture of the CFRP sheet can be seen as the sign of the failure of the combined structure.

Some mechanical properties of GFRP are sensitive to the stress state variation. So when the CFRP sheet confined GFRP short pole is axially compressed, the mechanical properties of the core GFRP will vary with the variation of the axial pressure and corresponding lateral pressure, and cause nonlinear response of the CFRP confined GFRP short pole. A theoretical iterative calculation approach for design and calculation of this kind of combined structure is suggested, and realized as computer program. The transverse isotropy and the nonlinearity in multiaxial stress state of the GFRP mechanical property is considered in this approach. This approach can be used to trace the variation of the stress and strain field and material mechanical property in CFRP sheet confined GFRP pole during the loading process, and finally attain the ultimate axial compressive stress of the combined structure. The theoretical results agree well with the experimental results.

The accuracy of the suggested calculation approach depends mostly on the adopted values of the GFRP mechanical parameters. The adopted mechanical parameters of the GFRP are calculated with the resin mechanical parameter formulas suggested by Birch and the FRP mechanical parameter composition formulas. The two groups of formulas are applicable to the FRP which is produced by good manufacturing process and of perfect mechanical properties. For FRP of poor manufacturing quality and poor mechanical properties, in order to ensure the accuracy of the calculation, it is necessary to attain its constitutive relations under different lateral pressures by experiment.

Though this research is based on the solid section GFRP pole, the results can be easily extended to a hollow section GFRP pole. And that work will be submitted in another paper.

## References

- Birch, F. (1938), "The effect of pressure upon the elastic parameters of isotropic solids, according to Murnaghan's theory of finite strain", *J. Appl. Phys.*, **9**, 279-288.
- Christiansen, A.W., Baer, E. and Radcliffe, S.V. (1971), "The mechanical behavior of polymers under high pressure", *Phil. Mag.*, **24**, 451-467.
- Fung, Y.C. (1994), *A First Course in Continuum Mechanics*, New Jersey, Prentice-Hall.
- Gonzalez, C. and Lorca, J.L. (2007), "Mechanical behavior of unidirectional fiber-reinforced polymers under transverse compression: Microscopic mechanisms and modeling", *Compos. Sci. Technol.*, **67**, 2795-2806.
- Hine, P.J., Deckett, R.A. and Kaddour, A.S. (2005), "The effect of hydrostatic pressure on the mechanical properties of glass fibre/epoxy unidirectional composites", *Composites: Part A*, **36**, 279-289.
- Hollaway, L.C. (2010), "A review of the present and future utilisation of FRP composites in the civil infrastructure with reference to their important in-service properties", *Construction and Building Materials Special Issue on Fracture, Acoustic Emission and NDE in Concrete (KIFA-5)*, **24**(12), 2419-2445.

- Hoppel, C.P.R. and Bogetti, T.A. (1995), "literature review-effects of hydrostatic pressure on the mechanical behavior of composite materials", *J. Thermoplast Compos.*, **8**, 375-409.
- Jones, R.M. (1975), *Mechanics of Composite Materials*, McGraw-Hill, New York.
- Juran, I. and Komornik, U. (2006), *Behavior of Fiber-Reinforced Polymer Composite Piles Under Vertical Loads*, Urban Utility Center of Polytechnic University, Brooklyn.
- Lam, L. and Teng, J.G. (2003), "Design-oriented stress-strain model for FRP-confined concrete", *Constr. Build Mater.*, **17**, 471-489.
- Pae, K.D. and Bhateja, S.K. (1975), "The effect of hydrostatic pressure on the mechanical behavior of polymer", *Journal of Macromolecular, Part C, Review in the Macromolecular Chemistry*, **13**, 1-75.
- Pae, K.D. and Sauer, J.A. (1970), *Influence of Pressure on the Elastic Modulus, the Yield Strength, and the Deformation of Polymers*, Aviemore, Scotland.
- Silano, A.A., Bhateja, S.K. and Pae, K.D. (1974), "Effects of hydrostatic pressure on the mechanical behavior of polymers: polyurethane, polyoxymethylene, and branched polyethylene", *Int. J. Polym. Mater.*, **3**, 117-131.
- Wang, X. and Wu, Z. (2010), "Evaluation of FRP and hybrid FRP cables for super long-span cable-stayed bridges", *Compos. Struct.*, **92**(10), 2582-2590.
- Wang, Z. (1991), *Composite Mechanics and Composite Structure Mechanics*, South China Technology University Press, Beijing.
- Weaver, C.W. and Williams, J.G. (1975), "Deformation of a carbon-epoxy composite under hydrostatic pressure", *J. Mater. Sci.*, **10**, 1323-1333.
- Woo, P.J., Kyun, H.Y. and Sung, C.M. (2010), "Behaviors of concrete filled square steel tubes confined by carbon fiber sheets (CFS) under compression and cyclic loads", *Steel Compos. Struct.*, **10**(2), 187-205.
- Wronski, A.S. and Parry, T.V. (1982), "Compressive failure and kinking in uniaxially aligned glass-resin composite under superposed hydrostatic pressure", *J. Mater. Sci.*, **17**, 3656-3662.
- Xiong, J., Ma, L., Wu, L., Wang, B. and Vaziri, A. (2010), "Fabrication and crushing behavior of low density carbon fiber composite pyramidal truss structures", *Compos. Struct.*, **92**(11), 2695-2702.
- Xu, Z. (1990), *Elastic Mechanics*, High Education Press, Beijing.
- Youakim, S.A. and Karbhari, V.M. (2007), "An approach to determine long-term behavior of concrete members prestressed with FRP tendons", *Constr. Build Mater.*, **21**(5), 1052-1060.
- Zhang, G., Liu, B., Bai, G. and Liu, J. (2009), "Experimental study on seismic behavior of high strength reinforced concrete frame columns with high axial compression ratios", *Struct. Eng. Mech.*, **33**(5), 653-656.
- Zhang, X. and Ou, J. (2006), "Experimental research on compressive properties of concrete stub square column reinforced with FRP bars", *J. Xi'an Univ. of Arch. & Tech.*, **4**, 467-472.
- Zinoviev, P.A., Tsvetkov, S.V., Kulish, G.G., van den Berg, R.W. and Van Schepdael, L.J.M.M. (2001), "The behavior of high-strength unidirectional composites under tension with superposed hydrostatic pressure", *Compos. Sci. Technol.*, **61**(8), 1151-1161.